Reconstruction of Spectral Images from the AEOS Spectral Imaging Sensor

Maj Travis F. Blake
Lt Col Matthew E. Goda
Dr. Stephen C. Cain
Air Force Institute of Technology
2950 Hobson Way, WPAFB, OH, 45433

Kenneth J. Jerkatis
Boeing SVS
4411 The 25 Way,Albuquerque, NM 87109

ABSTRACT

Spectral images of terrestial objects has provided a wealth of information beyond the tradidtional data in a panchromatic image. What has proven to be successful for terrestial applications, can also be applied to images of objects in space.

This research expands on previous work discussing the image processing for data collected by the new AEOS Spectral Imaging Sensor (ASIS). ASIS uses broadband filters to collect AO compensated spectral images of astronomical objects and satellites. The use of the broadband filters spectrally blurs the images collected by ASIS. A post-processing algorithm called Model-Based Spectral Image Reconstruction (MBSIR) can simultaneously remove much of the spatial and spectral blurring introduced by the sensor.

1. INTRODUCTION

Spectral images of terrestial objects has provided a wealth of information beyond the tradidtional data in a panchromatic image. What has proven to be successful for terrestial applications, can also be applied to images of objects in space.

This research expands on previous work discussing the image processing for data collected by the new AEOS Spectral Imaging Sensor (ASIS). ASIS uses broadband filters to collect AO compensated spectral images of astronomical objects and satellites. The use of the broadband filters spectrally blurs the images collected by ASIS. A post-processing algorithm called Model-Based Spectral Image Reconstruction (MBSIR) can simultaneously remove much of the spatial and spectral blurring introduced by the sensor.

This paper starts by briefly reviewing the development of the MBSIR algorithm. The paper then shows the benefit of the post-processing algorithm on data collected in a laboratory type set-up. In this configuration, ASIS was programmed to collect a spectral image of a reference test grid illuminated by a spectral source. The sensor parameters were set-up such that the spectral image was blurred both spatially and spectrally. The blurring causes spatial and spectral features in the test grid to be unresolvable. The application of the MBSIR algorithm to the data resolves these features.

2. SPECTRAL IMAGE RECONSTRUCTION

A complete derivation and discussion of the MBSIR algorithm is not included in this paper. Briefly described, the algorithm to reduce the spectral blurring in the images collected from ASIS is derived from a maximum likelihood (ML) estimator based on 1) the statistics of the light collection and 2) the imaging sensor [1]. The Deconvolution term referenced in the title of previous work was changed to Reconstruction to more accurately describe the algorithm. The final reconstruction iteration for the MBSIR algorithm is,

$$o^{new}(u_o, v_o, \gamma_o) = \frac{o^{old}(u_o, v_o, \gamma_o)}{\sum_{x,y,\lambda}[h_1(x-u, y-v, \gamma)h_2(\lambda, \gamma)]} \sum_{x,y,\lambda}[\frac{d(x,y,\lambda)}{i^{old}(x,y,\lambda)} h_1(x-u_o, y-v_o, \gamma_o)h_2(\lambda, \gamma_o)], \quad (1)$$

where,

$$i^{old}(x, y, \lambda) = \sum_{u,v,\gamma} o^{old}(u, v, \gamma) h_1(x-u, y-v, \gamma) h_2(\lambda, \gamma) \; . \qquad (2)$$

In equations (1) and (2), $o(u_o,v_o,\gamma_o)$ is the estimate of the three dimensional true spectral scene at any given point in the scene, $d(x,y,\lambda)$ is the collected data, and $i(x,y,\lambda)$ is the image based on the estimate of the scene and the model of the sensor. Additionally, $h_1(u,v,\gamma)$ and $h_2(\lambda,\gamma)$ are the spatial spread function and spectral mixing function. These functions describe the blurring, spatially and spectrally, and the spectral photon losses from the sensor. It is the h_1 and h_2 functions that hold the model of the sensor. Fig 1 gives a pictorial description of equations (1) and (2) and the MBSIR algorithm.

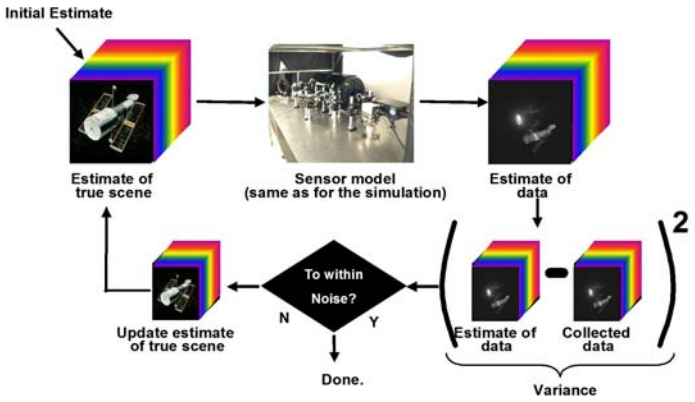

Fig 1: Pictorial description of the MBSIR algorithm.

3. AEOS SPECTRAL IMAGING SENSOR (ASIS)

As with the derivation of the MBSIR algorithm, a full description of ASIS is not included in this paper. A excellent description of the sensor is given in another paper in this conference. Briefly, ASIS is designed to collect spectral images of astronomical objects and satellites [2]. The sensor uses Liquid Crystal Tunable Filters (LCTFs) to spectral filter the light. ASIS is able to use the adaptive optics system to compensate for atmospheric blurring. A model of ASIS is used in the MBSIR algorithm to post-process the data. Fig 2 shows the layout of ASIS after the reduction telescope. The blue "cubes" in the figure, located in front of the cameras, are the LCTFs used in ASIS. It is the LCTFs that spectrally blur the data collected with ASIS. Through post-processing, some of this blurring can be

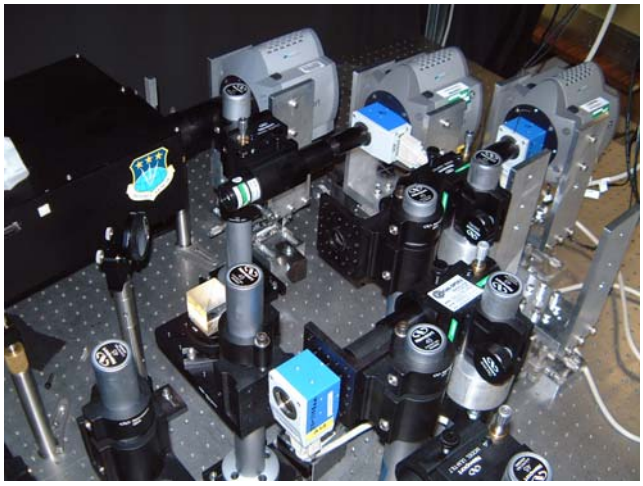

removed.

Fig 2: Layout of the AEOS Spectral Imaging Sensor (ASIS) after the reduction telescope.

4. DATA

ASIS was modified to collect the spectra of a Mercury-Argon (Hg(Ar)) Newport Spectral pencil lamp shown through a test grid. The collected data is similar to the data from a test bench constructed to prove the benefit of the MBSIR algorithm [3]. The spectral source was placed in the ASIS optical just after the reduction telescope. The test grid is shown in Fig 3 and the spectra of the Hg(Ar) source in Fig 4.

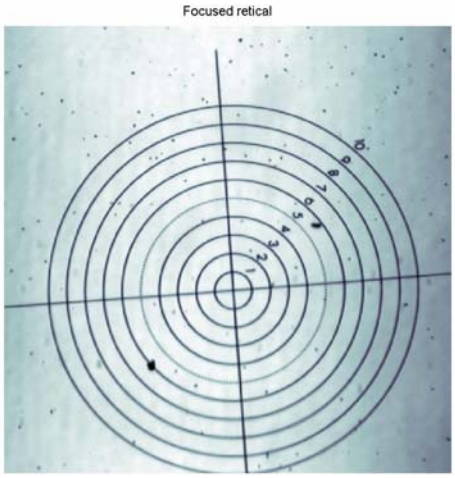

Fig 3: The test grid collected at a filter setting of 546nm.

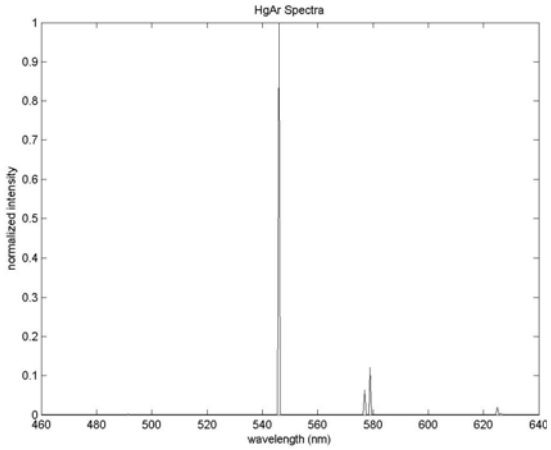

Fig 4: The spectra of the Hg(Ar) source.

The test grid illuminated with the spectral source was collected with a course spectral scan of the LCTF. The LCTF was programmed to collect an image of the grid at every 20nm from 480nm to 620nm. The coarse scan serves to blur the 546nm line and the 577/579nm lines so that the two lines are no longer resolvable in the spectra. The criteria used for the spectral resolution is based on the Rayleigh criteria. The spectral lines are resolved if the minimum between the two lines is less than 86% of the lower line intensity.

In addition to a course spectral scan, an intentional focus error is introduced so that spatial features in the test grid are also blurred together. In the test grid, the cross-section of the number 8 in the upper left of the grid will be used to demonstrate the spatial blurring. This section of the grid is shown in Fig 5, with the cross-section shown in Fig 6. In the figures, three distinct spatial features are seen. It is these three features that will be blurred with the focus error so that the features are not resolvable. The Rayleigh criteria will be used to determine the spatial resolution of the

spatial features. The goal of the MBSIR algorithm is then to reduce the spatial and spectral blurring such that the spatial features and spectral lines are again resolvable.

Fig 5: The section of the test grid containing the spatial features.

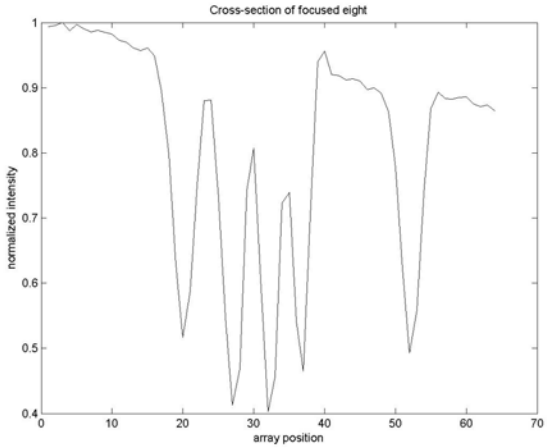

Fig 6: Cross-section of the test grid shown in Fig 5, showing the three spatial features.

Figures 7 and 8 show the test grid and cross-section of the test grid as collected with the known focus error. As seen in Fig 8, the three spatial features are not resolvable. Figure 10 shows the blurred spectra in the data due to the coarse 20nm filter sampling. In Fig 10, the spectral lines at 546nm and 577/579nm are not resolvable.

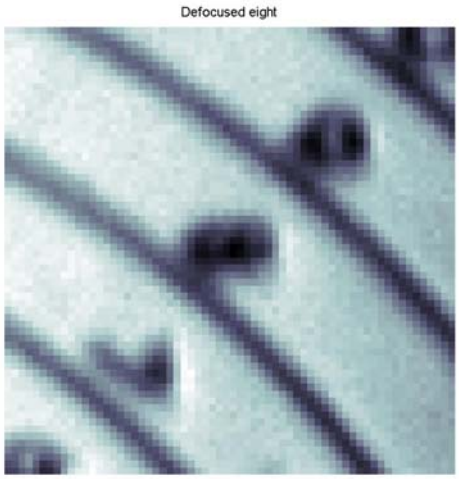

Fig7: Defocused section of the test grid containing the spectral features.

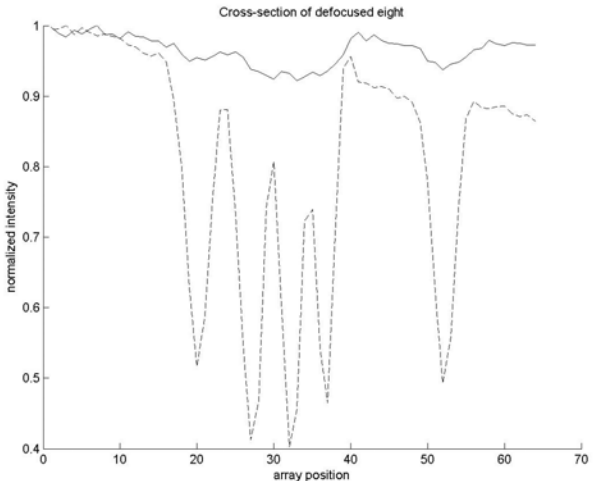

Fig 8: Cross-section of the defocused section of the test grid showing the blurred spectral features. The solid line is the blurred spectral features due to the focus error. The dashed lines show the focused spectral features.

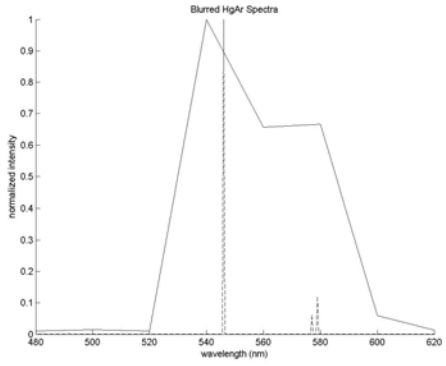

Fig 9: The blurred spectra due to the coarse 20nm filter scan. The solid line is the blurred spectra, the dashed lines are the spectral lines of Hg(Ar).

The collected data was then reconstructed with the MBSIR algorithm to simultaneously reduce both the spatial and spectral blurring. Figures 10 and 11 show the reconstructed spatial scene. In Fig 10, the number 8 can be seen, however it's not as clear as in the focused image in Fig 5. The cross-section shown in Fig 11 does show the three spectral features are clearly resolvable.

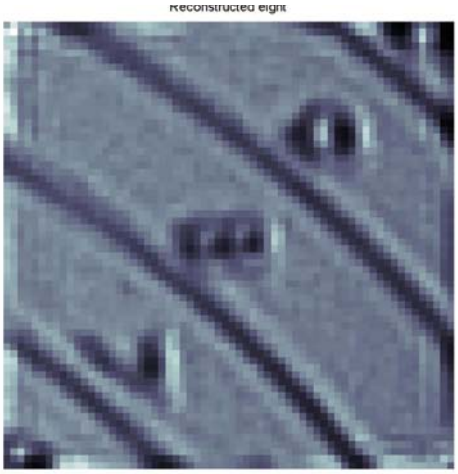

Fig 10: The reconstructed section of the test grid.

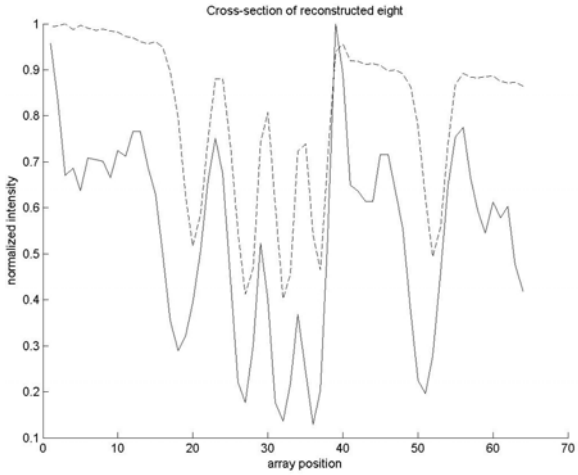

Fig 11: Cross-section of the reconstructed section of the test grid. The solid line shows the spatial features are now resolvable and compare well with the same features in the focused section of the test grid. The dashed line shows the focused spatial features.

Figure 12 shows the reconstructed spectra. In the figure, the spectral lines of Hg(Ar) at 546nm and 577/570nm are resolvable. However, the location of the resolved spectral features are different from the known lines of Hg(Ar). The 546nm line is reconstructed at 538nm and the 577/579nm line at 574nm, for an 8nm and 4nm location error. This location error can be improved if the filter sampling was shifted. Instead of a 20nm filter sampling starting at 460nm, the 20nm sampling was shifted such that the filter sampling started at 466nm. When the shifted data was reconstructed with the algorithm, the location error of the spectral features was reduced. Figure 13 shows the reconstructed spectra with the shifted 20nm filter sampling. As seen in the figure, the location error was reduced to 2nm for both spectral lines. The location error can also be reduced by using a finer filter sampling. A 5nm filter sampling was used in Figure 14 to demonstrate the reduced location error.

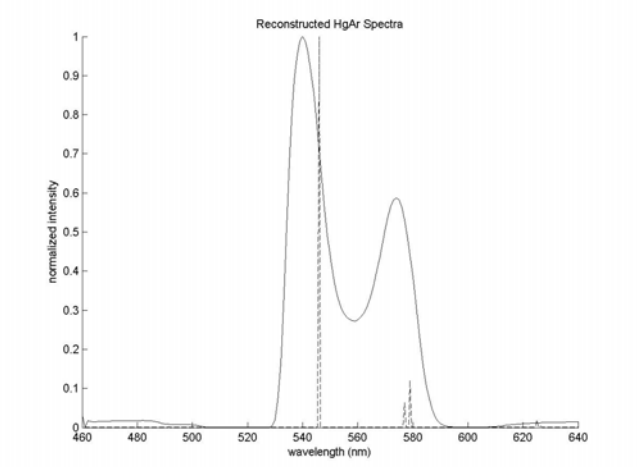

Fig 12: Reconstructed spectra of the Hg(Ar) spectral source. The solid line shows that the spectral lines at 546nm and 577/579nm are now resolvable, but are slightly shifted from the spectral lines of Hg(Ar), shown in the dashed lines.

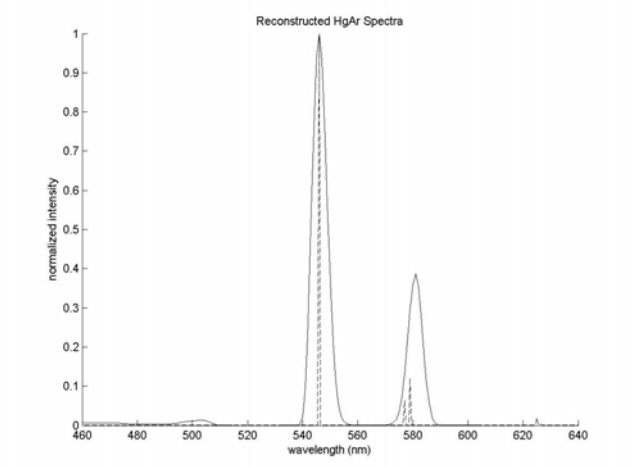

Fig: 13 Reconstructed spectra of the Hg(Ar) source with the shifted filter sampling. The solid line shows that the spectral lines at 546nm and 577/579nm are resolvable, and are closer to the spectral lines of Hg(Ar), shown in the dashed lines.

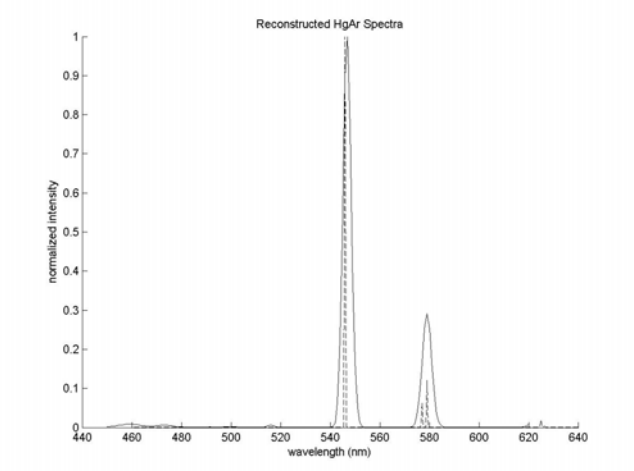

Fig: 14 Reconstructed spectra of the Hg(Ar) source with the finer 5nm filter sampling. The solid line shows that the spectral lines at 546nm and 577/579nm are resolvable, and are closer to the spectral lines of Hg(Ar), shown in the dashed lines.

5. SUMMARY

The AEOS Spectral Imaging Sensor has been constructed to collect spectral images of objects in space. To create a spectral image, ASIS utilizes liquid crystal tunable filters to filter the collected light. The bandwidths of the LCTFs spectrally blur the image. Using the MBSIR algorithm this spectral blurring can be reduced. In addition to reducing the spectral blurring, the MBSIR algorithm can simultaneously reduce any known spatial blurring in the image.

The MBSIR algorithm has been shown to reduce the spatial and spectral blurring in data collected in a laboratory set-up. The algorithm was able to resolve both spatial and spectral features in an image, where these features were not resolvable in the collected data.

6. REFERENCES

1. Blake, T. F., Cain S. C., Goda, M. E., and Jerkatis, K. J., "Spectral Image Deconvolution Using Sensor Models," *2005 SPIE Conference, Unconventional Imaging*, SPIE Vol. 5896
2. Blake, T. F., Cain S. C., Goda, M. E., and Jerkatis, K. J., "Model of the AEOS Spectral Imaging Sensor (ASIS) for Spectral Image Deconvolution," *2006 AMOS Technical Conference*
3. Blake, T. F., Cain S. C., Goda, M. E., and Jerkatis, K. J., "Enhancing the Resolution of Spectral Images," *2006 SPIE Defense and Security Symposium*, SPIE Vol. 6233

DISCLAIMER: Research sponsored in part by the Air Force Research Laboratory, Air Force Materiel Command, USAF. The United States Government is authorized to reproduce and distribute reprints notwithstanding any copyright notation thereon. The views and conclusions contained in this dissertation are those of the author and should not be interpreted as necessarily representing the official policies or endorsements, either expressed or implied, of the Air Force Research Laboratory, the United States Air Force, Department of Defense, or the United States Government.